

Application of topology optimization to bridge girder design

Ryszard Kutylowski^{*1} and Bartosz Rasiak^{2a}

¹*Institute of Civil Engineering, Wrocław University of Technology, Wyb. Wyspiańskiego 27, Poland*

²*Alpine Bau GmbH, Polish Branch, Poland*

(Received August 6, 2011, Revised March 15, 2014, Accepted May 1, 2014)

Abstract. This study deals with the design of bridge girder structures and consists of two parts. In the first part an optimal bridge girder topology is determined using a software based on structure compliance minimization with constraints imposed on the body mass, developed by the authors. In the second part, an original way in which the topology is mapped into a bridge girder structure is shown. Additionally, a method of converting the thickness of the bars obtained using the topology optimization procedure into cross sections is introduced. Moreover, stresses and material consumption for a girder design obtained through topology optimization and a typical truss girder are compared. Concluding, this paper shows that topology optimization is a good tool for obtaining optimal bridge girder designs.

Keywords: topology optimization; minimum compliance; design of bridge truss girders

1. Introduction

This paper combines two approaches: a theoretical approach and a practical engineering approach. On the one hand it deals with topology optimization, i.e. finding the optimal bridge girder topology and then determining the cross sections of the particular girder bars on the basis of the girder bar thicknesses obtained in the course of topology optimization. On the other hand, the topology which is transformed into a bridge girder is re-designed (checked) according to the current codes (Code 1, Code 2, Code 3). This means that this paper has also a practical character. A similar combination of theoretical and practical approaches was adopted in (Lee and Park 2011) for designing a truss girder and determining the size of the cross sections of its bars.

Conventional truss bridge designs are based on a simple bar system whereby bridge structures can be quite easily dimensioned and built. But it turns out that such structures are not always optimally designed. Therefore a study was undertaken to determine the optimal bridge girder shape, using the author's own algorithm and a program written in MATLAB, whose effectiveness and agreement with the results reported in the literature had been previously verified (Kutylowski and Rasiak 2008). Later in this paper it is demonstrated how topology optimization results can be used in the design process.

Generally, in this paper the following problems are considered:

*Corresponding author, Professor, E-mail: ryszard.kutylowski@pwr.edu.pl

^aPh.D.

- 1) finding the optimal bridge girder topology and its approximation to a bar structure,
- 2) determining the cross sections of the bars on the basis of the girder topology,
- 3) a comparison of the normalized cross sections of a typical truss girder with those of the girders obtained through topology optimization.

The topology optimization procedure leading to an optimal bridge girder design conforming to the current standards involves the following steps:

- 1) determination of optimal topologies;
- 2) transformation and approximation of the topologies to a bar structure,
- 3) determination of the (square and circular) solid cross sections (K, O) of the truss constructions for the assumed standard material specifications;
- 4) determination of the box and tubular sections (KS1, KS2, OR1, OR2) of the truss constructions for the outside overall bar dimensions used in bridge building;
- 5) adjustment of the size (size reduction) of the required cross section because of the overdimensioning required by the unification of overall dimensions (KS1', KS2', OR1', OR2'); the condition that the load capacity of the individual cross sections cannot be exceeded is applied here;
- 6) checking the local stability condition; since this condition was fulfilled in some cross section, it became necessary to increase the surface area of the cross sections.
- 7) the obtained topologies were used to approximate the cross-sectional area of the individual bars, then after normalizing the cross sections and the cross sections obtained from the previous calculations the agreement between the cross-sectional areas for the two cases was analyzed;
- 8) for solutions in points 5 and 6 separate quantitative analyses of material consumption were carried out to determine which of the truss designs was the most optimal.

Variational calculus was used to solve the topology optimization problem. Compliance was adopted as the objective functional. Its equivalent, i.e., energy of deformation, was minimized with constraints imposed on the mass of the body being optimized. The constraints satisfy this equation

$$H(\rho_j) = \frac{m_j}{m_0} - 1 = 0 \quad (1)$$

which means that for each successive optimization step j the body's mass must be equal to available mass m_0 defined as

$$m_0 = \alpha m, \quad 0 < \alpha < 1 \quad (2)$$

$$m = V \rho \quad (3)$$

where V is the design area volume, ρ is the density of the material to be used to design an optimal structure and α is a mass reduction coefficient (often referred to as a volume fraction coefficient). Thus the following objective functional is minimized

$$F(\rho(x)) = \min \left\{ \int_{\Omega} C^{ijkl}(\rho(x)) e_{ij} e_{kl} d\Omega; \quad \bigwedge_{x \in \Omega} \rho(x) \in R^+; \quad \int_{\Omega} \rho_x d\Omega = m_0 \right\} \quad (4)$$

where ρ_x is an arbitrary body density in point with coordinate x , and λ is a Lagrange multiplier. Young's modulus was updated using the relation

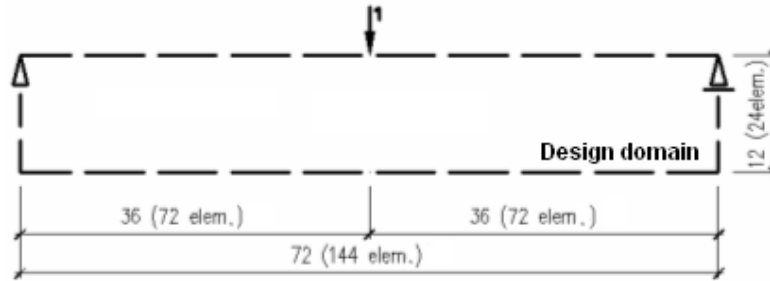


Fig. 1 Analyzed design domain

$$E = E_0 \left(\frac{\rho_j^i}{\rho} \right)^p \quad (5)$$

where ρ is the density of the material from which the structure is to be made and ρ_j^i is the body material density in point i for step j .

Generally, this study is based on the *artificial density approach* (Bendsøe 1989, Ramm *et al.* 1994, Bendsøe and Sigmund 1999, Bendsøe and Sigmund 2003).

The finite element method, where a finite element corresponds to a material point, was used for the numerical solution. Appropriate problem controlling parameters were adopted. Previously, their effectiveness, ensuring that the optimum topology is obtained in the possibly smallest number of optimization steps (Kutyłowski and Rasiak 2008), had been checked. The optimum topology is understood to be a topology with minimum or nearly minimum deformation energy. Since the aim was to obtain a 0/1 distribution, it is often the case that such a topology is characterized by strain energy not much greater than the minimum one, i.e. the structure is then “nearly optimal”.

2. Determination of optimal bridge girder topology and its approximation to bar structure

The design area with the assumed boundary conditions and the load is shown in Fig. 1. The freely supported area in the design area’s upper corners constitutes a static scheme. A unit force is applied to the design area’s top edge at its midspan. The proposed scheme corresponds to a deck bridge and the load corresponds to the most disadvantageous load as regards load influence lines.

The 72×12 [m] design area was divided into 0.5×0.5 [m] rectangular finite elements. In total there were 144×24 elements. The available mass was assumed to amount to 0.5 of the total mass ($\alpha=0.5$). The material was steel.

Computations were performed using the algorithm and the program written in Matlab (Kutyłowski and Rasiak 2008). The SIMP method and power exponents equal to 1 and 2 were employed. It should be mentioned that recently instead of formula (5) polynomials have been employed (Niu *et al.* 2009). After relation (5) had been applied in the algorithm, threshold function $FP=0.02*nr$, where nr is the number (at a given instant) of the analyzed optimization step, was additionally used to penalize relatively small densities. It should be noted that on the basis of the threshold values used in (Guedes and Taylor 1997) threshold functions were defined and used in

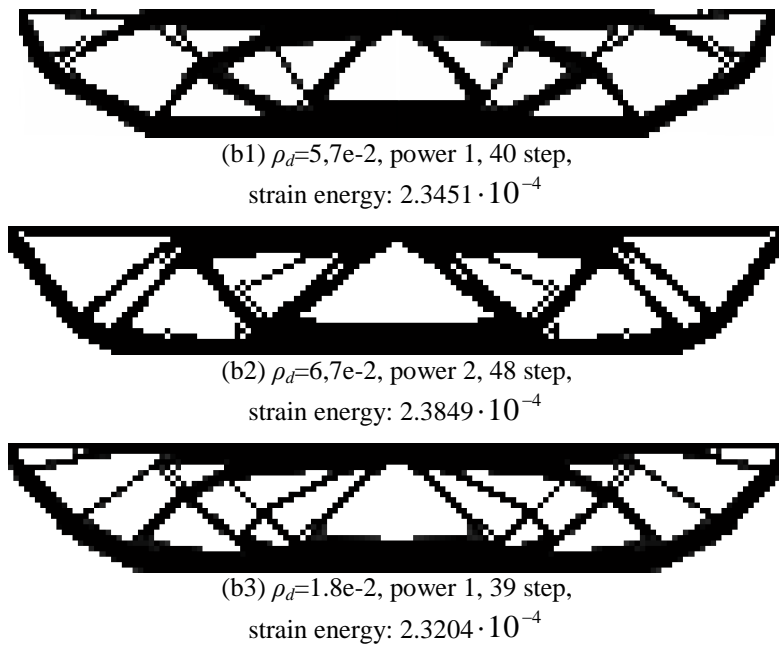


Fig. 2 Optimal topologies for deck girder

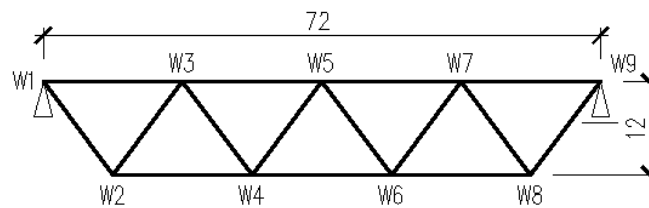
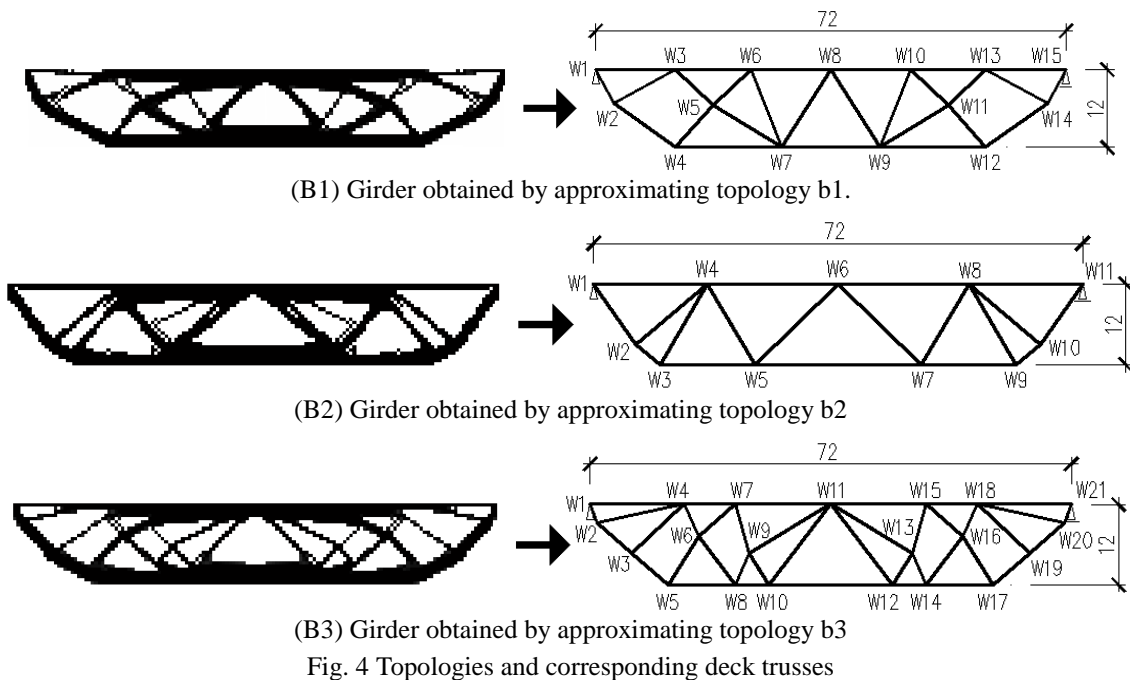


Fig. 3 Reference truss girder (A)

(Kutylowski 2002) and in (Kutylowski and Rasiak 2008). The aim of the functions was to aid the process leading to a 0/1 solution. Moreover, the algorithm procedure ensuring the fulfilment of the mass constancy condition, required the use of a limit density value below which no mass make up (ρ_d) would be used. This parameter was also used (in the same way) for penalization with the threshold function. The choice of the optimization control quantities was dictated by the effectiveness of the parameters.

From among the obtained topologies three results with the lowest strain energy, denoted respectively b1, b2 and b3 (Fig. 2), were chosen for further analysis. Thanks to the choice of not one, but three topologies it was possible to make a wide comparative analysis for energywise close topologies. Fig. 2 includes the values of some control parameters and the number of the optimization step in which the given topology was obtained. Strain energy values are shown for each topology separately. The lowest energy values were obtained for topology b3 while the other energy values are close to the minimum value. One should add here that the designated quantities after proper transformations are ultimately written as dimensionless quantities.

The structure (whose dimensions can be inscribed into the design area demarcated in Fig. 1) shown in Fig. 3 was used as a reference (typical) deck truss bridge structure. The figure also shows



the numbering scheme adopted for the nodes in this truss.

Having determined the topologies one should properly transform and approximate them into bar structures. The aim is to possibly faithfully map the topologies into bar structures while making some approximations aiding certain stages of the postprocessing included in the optimization procedures and simplifying sometimes the too complicated scheme of connecting bars in the bar structure being mapped. Truss B1 bar W1-W3 and the location of node W4 in truss B2 are examples of the result of such operations.

All the bar structure models (B1, B2, B3) built from one-dimensional elements in a two-dimensional space are referred to as class (e^1, p^2) models. Such a description of a design space and finite elements is commonly used in bridge construction (Kmita *et al.* 1989), also for truss bridge structures.

The central axes of the individual bars intersecting in the nodes in the topologies are determined using the graphic approach. However, sometimes some nodes were combined into one node in order to simplify the analyzed structure topology (e.g., for truss B3 bar W1-W4). In this way the bar structures (denoted by capital letters B1, B2 and B3) for respectively topology b1, b2 and b3) shown on the right in Fig. 4 were obtained. The bars were assumed to be one-dimensional elements. Because of the adopted design area height the axial spacing between the top flange and the bottom flange was set to 12 m.

3. Adopted load and cross sections of structure

In order to obtain results closest to the real ones, a standard load acc. to (Code 1) was adopted. It was assumed that the location of the heaviest load at midspan corresponded to a loading scheme

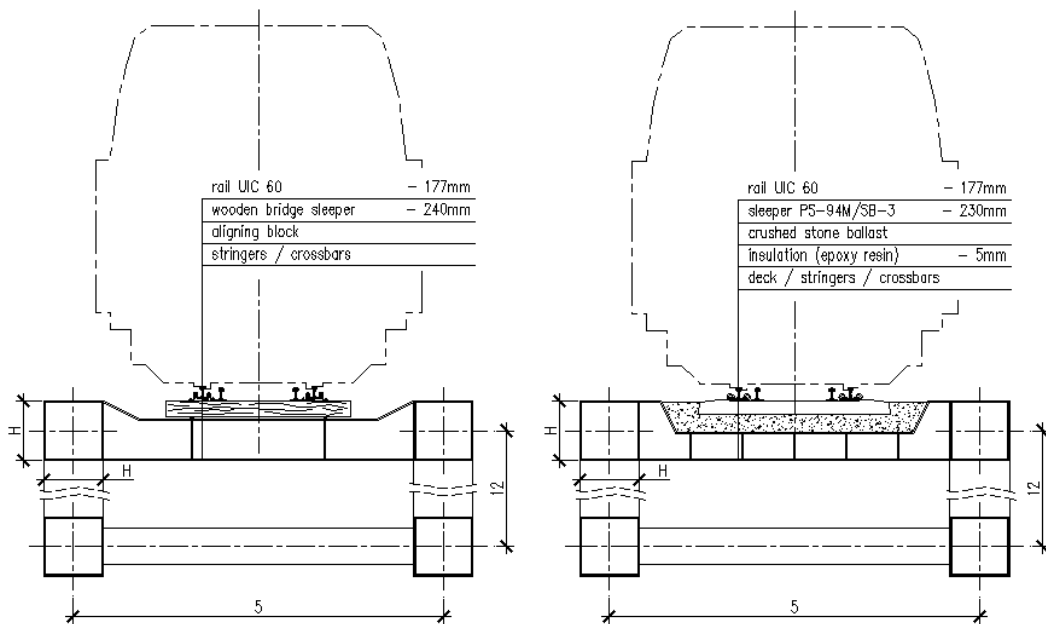


Fig. 5 Types of deck: open (a) and closed (b)

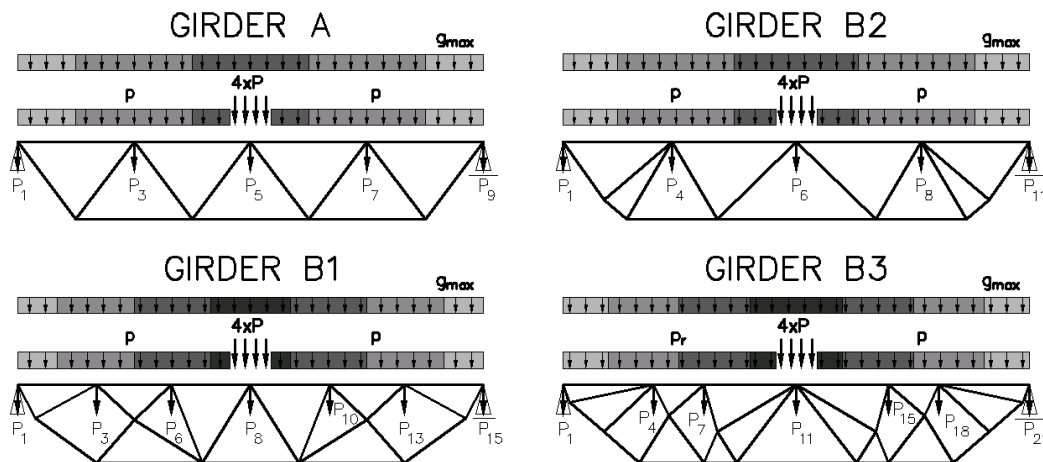


Fig. 6 Loading of analyzed girders

with a unit force located in the middle of the designed area's top edge (Fig. 1). The considered single girder is one of the two girders constituting a railway bridge structure. The girders support a deck on which trains run. An open deck (seldom used today) (Fig. 5(a)) and a closed deck (currently commonly used) were assumed. When assuming the loads, the girder design and the cross sections, care was taken that they corresponded to the actual ones used in bridge building today in order to make this work as applicable as possible from both the scientific and engineering points of view. A static truss scheme with load transferred in nodes was adopted.

The loads were calculated in accordance with (Code 1), which means that the following loads act on a single girder:

Table 1 Forces loading truss girders A, B1, B2 and B3

| Truss A | | | | |
|-----------------|--------|---------|-----------------|------------|
| Force | P [kN] | p [kN] | g_{\max} [kN] | TOTAL [kN] |
| $P_1=P_9$ | 0 | 653.40 | 433.86 | 1087.26 |
| $P_3=P_7$ | 0 | 1306.80 | 867.71 | 2174.51 |
| P_5 | 907.50 | 842.16 | 867.71 | 2617.37 |
| Truss B1 | | | | |
| Force | P [kN] | p [kN] | g_{\max} [kN] | TOTAL [kN] |
| $P_1=P_{15}$ | 0 | 444.68 | 295.26 | 739.94 |
| $P_3=P_{13}$ | 0 | 862.13 | 572.45 | 1434.57 |
| $P_6=P_{10}$ | 0 | 862.13 | 572.45 | 1434.57 |
| P_8 | 907.50 | 424.71 | 590.53 | 1922.74 |
| Truss B2 | | | | |
| Force | P [kN] | p [kN] | g_{\max} [kN] | TOTAL [kN] |
| $P_1=P_{11}$ | 0 | 608.03 | 403.73 | 1011.75 |
| $P_4=P_8$ | 0 | 1306.80 | 867.71 | 2174.51 |
| P_6 | 907.50 | 932.91 | 927.97 | 2768.38 |
| Truss B3 | | | | |
| Force | P [kN] | p [kN] | g_{\max} [kN] | TOTAL [kN] |
| $P_1=P_{21}$ | 0 | 508.20 | 337.44 | 845.64 |
| $P_4=P_{18}$ | 0 | 789.53 | 524.24 | 1313.77 |
| $P_7=P_{15}$ | 0 | 798.60 | 530.27 | 1328.87 |
| P_{11} | 907.50 | 569.91 | 686.94 | 2164.35 |

- railway rolling stock load (locomotive): $4 \times P = 226.88$ kN,

- railway rolling stock load (rail coaches): $p = 72.60$ kN/m,

- the weight of the deck, the track superstructure and the insulation: $g_{\max} = 48.21$ kN/m.

The above loads were assumed to be transferred by collecting the forces into the nearest node.

The loading schemes for the particular types of girders are shown in Fig. 6.

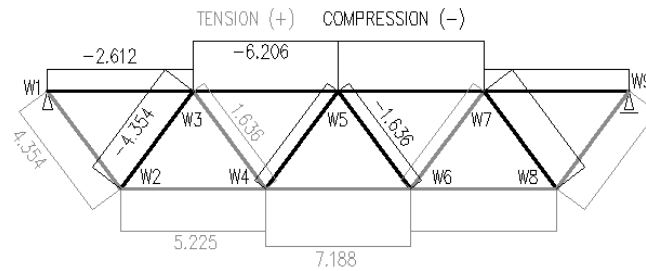
The loading forces in the particular nodes of the analyzed trusses are shown in Table 1. The numbers of the forces correspond to the numbers of the nodes in which they were applied.

The static calculations yielded values [MN] of the internal (axial, tensile and compressive) forces, which are shown in the diagrams in Fig. 7. The tensile and compressive forces are marked respectively shade of grey and black.

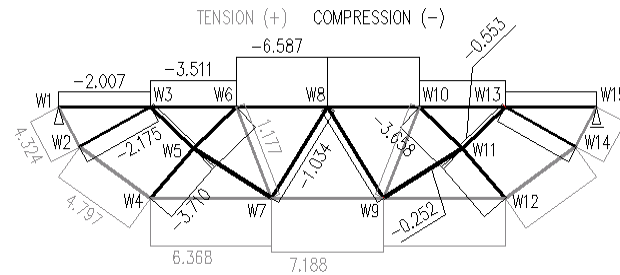
For further calculations it was assumed that the structure would be made of steel with design strength $R = 200$ MPa. The allowable (according to (Code 2)) slenderness for compressed and tensioned elements is respectively $\lambda_{\max} = 150$ and $\lambda_{\max} = 200$.

The above three conditions determined the amount of material in each of the truss bars. In cases when the allowable slenderness was exceeded, the material was added to reach the limit value. In the other cases, strength R of the steel was the determining factor.

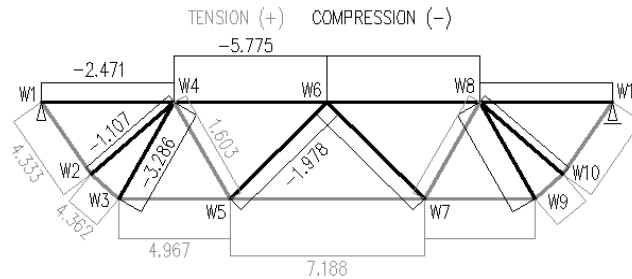
Different types of cross sections of the individual bars were analyzed to ensure a wide analytical range. Initially, under more rigorous conditions for steel strength and allowable element slenderness, the amount of required material was determined for solid cross sections: square (K) and circular (O) (Fig. 8). The cross sections were then referred to as *initial*. The dimensions of K



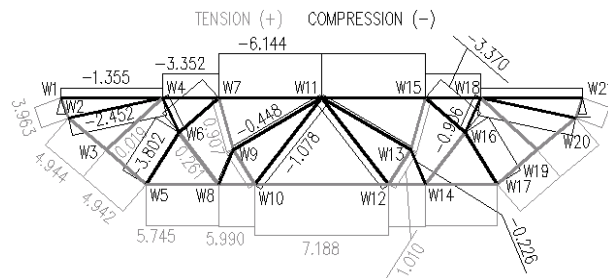
(A) Typical truss girder.



(B1) Girder obtained by approximating topology b1.



(B2) Girder obtained by approximating topology b2.



(B3) Girder obtained by approximating topology b3.

Fig. 7 Axial forces for analyzed trusses [MN]

and O (respectively the side of a square and the diameter) are different for each bar and depend on the axial force acting in it.

Then the material determined for the *initial cross sections* was shifted away from the cross section's geometric centre to the outside, whereby square box sections KS1, KS2 and circular tube sections OR1, OR2 (Fig. 8), further referred to as *constant sections*, were formed. The amount of steel for sections KS1, KS2 and OR1 and OR2 was respectively the same as for sections K and O,

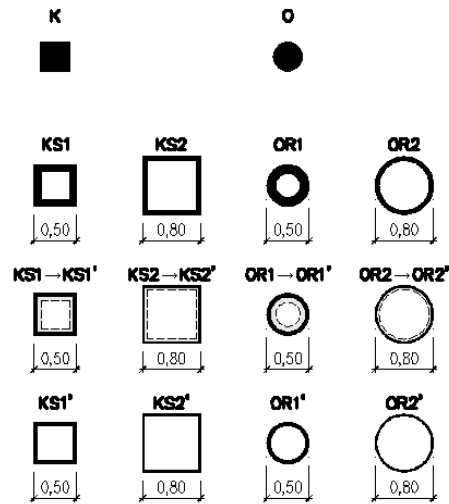


Fig. 8 Adopted truss bar cross sections

which means that the amount of material in the course of shifting was constant. The outside dimensions of the newly formed sections were fixed at 0.50 m (KS1, OR1) and 0.80 m (KS2, OR2). The dimensions correspond to the outside dimensions of the cross sections of steel spans having the considered span length and height, used in bridge building and they will be further referred to as overall dimensions. This way of bar dimensioning was used in the further shaping of the structures. The cross sections determined in this way were often found to be oversized which meant that in the next step the superfluous mass had to be removed from box sections KS1, KS2 and tubular sections OR1, OR2. Only such an amount of mass could be removed that the strength and slenderness conditions remained satisfied. In this way optimally designed cross sections KS1', KS2', OR1', OR2' having different thickness in the particular bars were obtained. The cross sections are further referred to as *reduced cross sections*.

4. Stress and critical forces analysis of individual girders

The initial steps of the algorithm which will be used to build (through topology optimization) an optimal bridge girder structure conforming to the current standards are described in this section.

Computations were performed for the particular trusses: the typical one (A) and the ones approximated from the individual topologies (B1, B2, B3) for all the cross sections. Selected results of the computations are presented in the tables below. The values shown in grey are for the tensioned bars while the ones shown in black are for the compressed bars (denoted by minus). The first four tables show results for only truss A and B1 for the square cross sections. The same trends as here are observed in the other cases.

The previously determined axial forces in the bars of the girders were used to calculate the stresses in respectively the tensioned and compressed bars. A buckling coefficient m_w (Code 2) was taken into account when calculating stress for the compressed bars. The coefficient includes the randomness of the material characteristics and the probability of occurrence of all kinds of imperfections. The buckling length for the top flange, the bottom flange and the support diagonal

Table 2 Stresses in bars of truss A – cross sections K, KS1, KS2

| Element | Section K | Section KS1 ($H=0.50$ m) | Section KS2 ($H=0.80$ m) |
|---------|----------------|------------------------------|------------------------------|
| | σ [MPa] | σ [MPa] | σ [MPa] |
| W1-W2 | 64.50* | 64.50 | 64.50 |
| W2-W4 | 53.75* | 53.75 | 53.75 |
| W4-W6 | 73.95* | 73.95 | 73.95 |
| W1-W3 | -48.68* | -26.30 | -17.84 |
| W3-W5 | -115.65* | -62.49 | -42.38 |
| W2-W3 | -182.55* | -68.03 | -61.79 |
| W3-W4 | 37.87* | 37.87 | 37.87 |
| W4-W5 | -68.59* | -25.56 | -23.22 |

“+” represents tension and “-” stands for compression

* – slenderness taken into account: $\lambda=200$ (tension) and $\lambda=150$ (compression)

Table 3 Stresses in bars of truss B1 – cross sections K, KS1, KS2

| Element | Section K | Section KS1 ($H=0,50$ m) | Section KS2 ($H=0,80$ m) |
|---------|----------------|------------------------------|------------------------------|
| | σ [MPa] | σ [MPa] | σ [MPa] |
| W1-W2 | 200.00 | 200.00 | 200.00 |
| W2-W4 | 117.73* | 117.73 | 117.73 |
| W4-W7 | 80.39* | 80.39 | 80.39 |
| W7-W9 | 106.48* | 106.48 | 106.48 |
| W1-W3 | -80.73* | -30.34 | -27.33 |
| W3-W6 | -160.26* | -59.23 | -53.75 |
| W6-W8 | -200.00 | -86.83 | -77.58 |
| W2-W3 | -174.18* | -60.04 | -57.34 |
| W3-W5 | -82.43* | -27.39 | -26.62 |
| W4-W5 | -200.00 | -101.89 | -98.12 |
| W5-W6 | -200.00 | -109.18 | -106.12 |
| W5-W7 | -15.58* | -5.52 | -5.18 |
| W6-W7 | 36.79* | 36.79 | 36.79 |
| W7-W8 | -48.70* | -17.85 | -16.33 |

“+” represents tension and “-” stands for compression

* – slenderness taken into account: $\lambda=200$ (tension) and $\lambda=150$ (compression)

was assumed (in accordance with the standard) to be equal to 1.0, and to 0.8 for the inner diagonal braces.

Table 2 shows stress values for sections K, KS1 and KS2 in real truss A. It is obvious that the stresses in the compressed cross sections of trusses KS1 (the overall dimension – 0.8 m) are lower than in the compressed cross sections of truss K. Nevertheless, these results are included here to complete the analysis presented later. It is apparent that the limit slenderness condition had to be taken into account for cross sections K in the compressed and tensioned bars. This is indicated by an asterisk. In the case when the bar’s slenderness meets the standard requirements, the decisive

Table 4 Axial forces and critical forces in bars of truss A, sections K, KS1, KS2

| Element | P (tension) | Section K P_{kr} [MN] | Section KS1 P_{kr} [MN] | Section KS2 P_{kr} [MN] |
|---------|--|----------------------------|------------------------------|------------------------------|
| | P^*m_w (compression) K / KS1 / KS2 [MN] | | | |
| W1-W2 | 4.35 | - | - | - |
| W2-W4 | 5.22 | - | - | - |
| W4-W6 | 7.19 | - | - | - |
| W1-W3 | 8.41 / 4.55 / 3.08 | 15.16 | 28.71 | 97.14 |
| W3-W5 | 19.98 / 10.80 / 7.32 | 15.16 | 28.71 | 97.14 |
| W2-W3 | 14.02 / 5.22 / 4.75 | 6.74 | 37.13 | 105.56 |
| W3-W4 | 1.64 | - | - | - |
| W4-W5 | 5.27 / 1.96 / 1.78 | 6.74 | 37.13 | 105.56 |

criterion is the design strength of the steel. The results of similar calculations for truss B are shown in Table 3.

Similarly as in (Lee and Park 2011), also the critical (Euler) forces for the particular bars were calculated from formula (6), and in this case they were compared with those in the compressed bars (Tables 4 and 5).

$$P_{kr} = \frac{\Pi^2 EI}{L_w^2} \quad (6)$$

The tensile force values and the compressive force values (with the buckling coefficient taken into account) are shown (on the basis of Fig. 7) in the second column in Table 4. The next three columns show the critical Euler force values calculated from formula (6). Let us examine Table 4: for bar W3-W5 (section K) the force equal to 19.98 MN is greater than $P_{cr}=15.16$ MN, which means that the square solid cross section does not meet the buckling capacity condition. This changes when section KS1 is used. Then there is even a quite large load capacity margin since the critical force of 28.7 MN is greater than the compressive force in the bar, equal to 10.80 MN.

The percentage increase in the load capacity of the individual bars when section K is replaced by KS1 or KS2, expressed by capacity to carry greater axial force loads (as follows from the strength condition or the critical force nonexceedance condition), for some bars of truss B1, and also truss B3 (as shown by similar calculations as for truss B1), is larger than for truss A. This means that the two structures obtained through optimization are really “better” than conventional trusses, such as truss A. The same trends were observed for the tubular sections.

Some exemplary comparisons of critical forces for the top flange in the individual trusses (A, B1, B2, B3) for the square solid sections (K) and box sections (KS1, KS2) are presented below.

For the *initial cross sections* (K) the critical force in the top flange elements amounts to 15.16 MN (A – Tab. 4), 7.02-9.39 MN (B1 – Tab. 5), 13.13-17.34 MN (B2) and 4.77-9.50 MN (B3). It is apparent that when solid cross sections are used in trusses B1 and B3, the critical force values are lower than for A and B2.

When box sections (KS1) were used, the critical force values calculated from Euler’s formula increased, amounting to respectively: 28.71 MN (A), 36.84-41.33 MN (B1), 26.53-30.74 MN (B2), 34.37-52.38 MN (B3). In this case, the force values for trusses B1 and B3 are higher than for A and B2.

Table 5 Axial forces and critical forces in bars of truss B1, sections K, KS1, KS2

| Element | P (tension) | Section K P_{kr} [MN] | Section KS1 P_{kr} [MN] | Section KS2 P_{kr} [MN] |
|---------|--|----------------------------|------------------------------|------------------------------|
| | P^*m_w (compression) K / KS1 / KS2 [MN] | | | |
| W1-W2 | 4.32 | - | - | - |
| W2-W4 | 4.80 | - | - | - |
| W4-W7 | 6.37 | - | - | - |
| W7-W9 | 7.19 | - | - | - |
| W1-W3 | 6.46 / 2.43 / 2.19 | 7.02 | 36.84 | 105.27 |
| W3-W6 | 11.30 / 4.18 / 3.79 | 6.19 | 37.68 | 106.11 |
| W6-W8 | 18.51 / 8.04 / 7.18 | 9.39 | 41.33 | 120.46 |
| W2-W3 | 7.00 / 2.41 / 2.31 | 3.53 | 40.34 | 108.77 |
| W3-W5 | 1.78 / 0.59 / 0.58 | 1.90 | 41.97 | 110.40 |
| W4-W5 | 7.86 / 4.01 / 3.86 | 5.28 | 61.82 | 166.49 |

For larger cross sections (KS2) the difference in critical force values favours structures B1 and B1 even more. Similar results were obtained for the circular solid sections (O) and the tubular section (OR1, OR2).

As the distance of the material from the geometric centre increases, the top flange elements of trusses B1 and B3 become increasingly optimal in comparison with truss A. Structures B1 and B3 are capable of carrying greater loads (P_{cr}) and much less material is needed to build them. Slightly worse in this respect is truss B2.

In the case of the compressed elements of all the trusses (A, B1, B2, B3) when the initial cross sections (K, O) are used, the critical force values calculated from Euler's formula are sometimes lower than the loading force values (e.g., bar W3-W6 in truss B1; $P m_w=11.30$ MN to $P_{kr}=6.19$ MN for sections K). When the initial cross sections were replaced by box sections (KS1) and tubular sections (OR1), this phenomenon did not occur.

5. Topology-based adoption of cross sections and comparison of normalized cross sections for typical truss and trusses obtained through topology optimization

The above analysis forms the basis for comparing cross sections with the ones obtained through topology optimization. For this purpose, a proper conversion should be performed so that suitable cross sections can be adopted for the individual bars in a fixed way. This was done as follows. Each of the bars was considered separately. Therefore each bar in Figure 9 was assigned a different shade of gray to distinguish it from the whole structure. Thanks to this the finite elements of each bar were distinguished. Then each bar's finite elements were divided by its design length (measured from node to node). As a result, averaged areas of the cross sections were determined for the particular bars. Then the area values were normalized and shown in the tables and figures below. Also in (Lee and Park 2011) a topology was the basis for determining cross-sectional areas. The thickness of the bridge girder deck bars was assumed proportionally to the thickness of the particular topology bars. The transformation (conversion) presented below is a little bit similar, but still different.

For example, if as the length of bar W4-W7 one assumes a length converted to the design

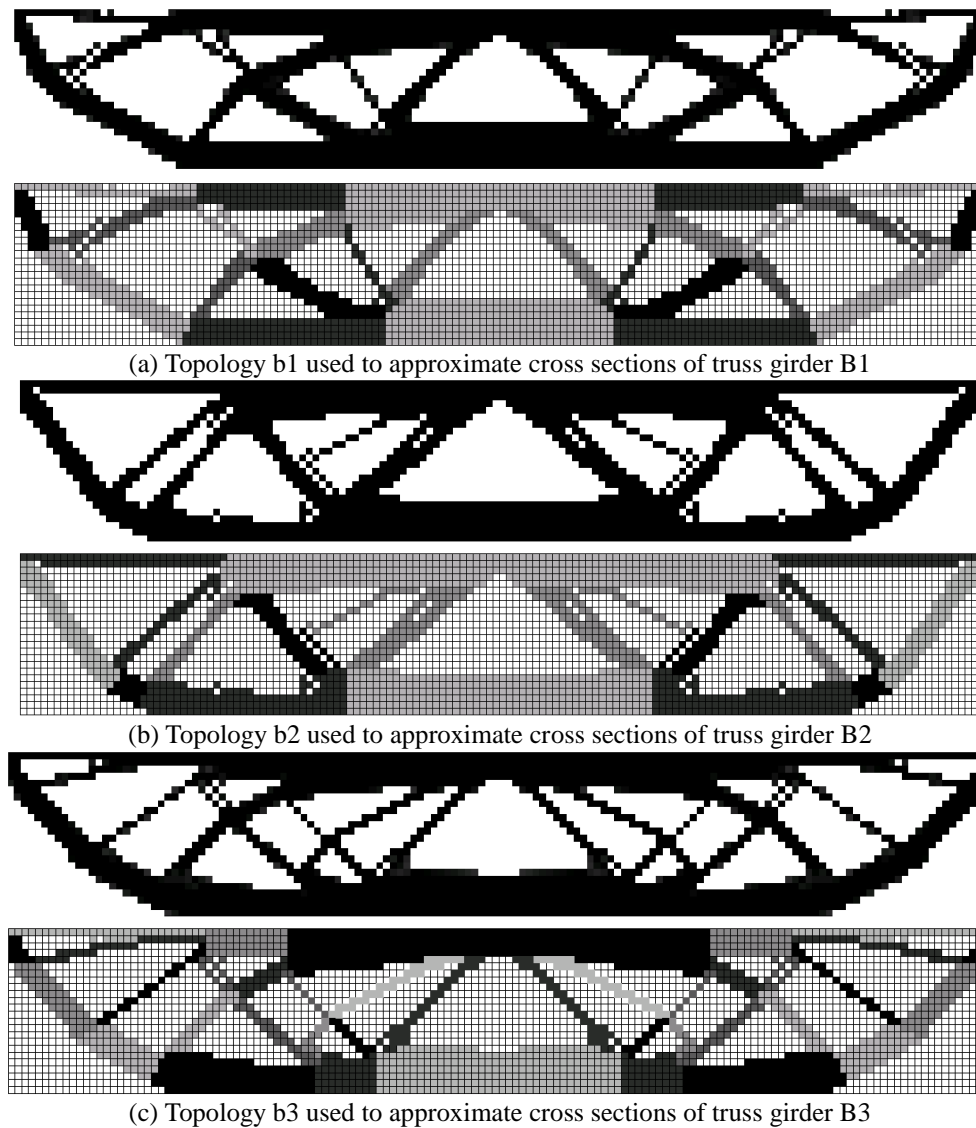


Fig. 9 Shade of grey marked elements of trusses B1, B2 and B3 on basis of topologies b1 (a), b2 (b) and b3 (c)

length (16.25 m), than the thickness of the bar is defined as the total number of finite elements per bar divided by the bar's design length, i.e., 118 elements/16.25 m. It should be noted that the bar's length of 16.25 m is the length measured between two nodes in the bar's axis. This length was read off figure 4. The highest value was obtained in the same way for bar W7-W9, by calculating: 230 elements/15 m. Then the values were normalized and the values of 1.0 and 0.47 were obtained for respectively bar W7-W9 and bar W4-W7. In this way the proportions of the cross sections in all the bars of all the trusses were determined.

It should be noted that in the case of a bar structure, topology optimization affects the cross sectional area values since a lot depends here on the design lengths of the particular truss bars. Nodes were identified by searching their location at the intersection of the axes of the topology

Table 6 Normalized cross-sectional area values for elements of topology b1 and for corresponding bars in structure B1

| Element | Topology b1 | <i>Initial and constant cross sections</i> | | <i>Reduced cross sections</i> | | | |
|------------------------------|----------------|--|--------------------|-------------------------------|-------------|--------------------|--------------------|
| | | K, KS1, KS2 | O, OR1, OR2 | KS1' | KS2' | OR1' | OR2' |
| W1-W2 | 0.31 | 0.23 | <u>0.23</u> | 0.55 | 0.60 | <u>0.52</u> | <u>0.59</u> |
| W2-W4 | 0.51 | 0.44 | <u>0.45</u> | 0.61 | 0.67 | <u>0.58</u> | <u>0.66</u> |
| W4-W7 | 0.47 | 0.86 | <u>0.88</u> | 0.81 | 0.89 | <u>0.77</u> | <u>0.87</u> |
| W7-W9 | 1.00 | 0.73 | <u>0.75</u> | 0.91 | 1.00 | <u>0.87</u> | <u>0.98</u> |
| W1-W3 | 0.19 | 0.86 | <u>0.89</u> | 0.30 | 0.30 | <u>0.30</u> | <u>0.30</u> |
| W3-W6 | 0.48 | 0.76 | <u>0.78</u> | 0.52 | 0.53 | <u>0.52</u> | <u>0.53</u> |
| W6-W8 | 0.71 | 1.00 | <u>1.00</u> | 1.00 | 1.00 | <u>1.00</u> | <u>1.00</u> |
| W2-W3 | 0.29 | 0.43 | <u>0.45</u> | 0.30 | 0.32 | <u>0.30</u> | <u>0.32</u> |
| W3-W5 | 0.16 | 0.23 | <u>0.24</u> | 0.07 | 0.08 | <u>0.07</u> | <u>0.08</u> |
| W4-W5 | 0.20 | 0.42 | <u>0.43</u> | 0.51 | 0.54 | <u>0.49</u> | <u>0.53</u> |
| W5-W6 | 0.38 | 0.39 | <u>0.39</u> | 0.50 | 0.53 | <u>0.48</u> | <u>0.52</u> |
| W5-W7 | 0.33 | 0.56 | <u>0.58</u> | 0.04 | 0.04 | <u>0.04</u> | <u>0.04</u> |
| W6-W7 | 0.09 | 0.35 | <u>0.36</u> | 0.15 | 0.16 | <u>0.14</u> | <u>0.16</u> |
| W7-W8 | 0.21 | 0.74 | <u>0.76</u> | 0.15 | 0.16 | <u>0.15</u> | <u>0.16</u> |
| Steel vol. [m ³] | - | 17.16 | 17.86 | 5.44 | 5.25 | 5.55 | 5.29 |

elements, assuming the spacing between the top and bottom flange to be equal to 12.0 m. One should note that the design lengths are not equal to the actual ones. Gusset plate size has a bearing on the way in which length should be taken into account. The actual lengths are shorter because of the large nodes in the joints in the topologies, which affects the actual buckling lengths. A similar trend is clearly visible in each of the analyzed topologies, where nodes are brought into interaction and material is accumulated in their vicinity. However, in many cases this results in difficulties in assigning a proper length (and so a cross section) to a given bar.

It should be noted that for truss A, internodal lengths are the real design lengths, whereas for all the B trusses the real design lengths are as a rule shorter because of the large nodes. This greatly affects the further calculations.

The bar thicknesses for the structures obtained through topology optimization were used to determine the size of the cross section. Let us remind ourselves that the topology had been determined within a 72×12 m design area divided into 144×24 elements (the finite element dimensions were 0.5×0.5 m). The choice of a finite element size is of consequence for determining the size of the cross section. For example, for the bar corresponding to bar W4-W7 near node W7 the number of elements is four. It is apparent that the dimension which would define the size of the bar cross section side does not correspond to the one actually used in practice and it can only serve as a relative measure. The real cross sections of the bars and the nodes are somewhat overscaled here. One should note that the cross sections of the topology bars are solid. Thus it makes sense to consider only the normalized sizes of bar cross sections. Nodes in a topology are larger than the ones used in practice. Nevertheless, their shape resembles that found in engineering solutions and, most importantly, when one examines the shape of the nodes it becomes apparent that the topology optimizing algorithm distributes the material in such a way as to minimize stress concentration and ensure most uniform stress distribution.

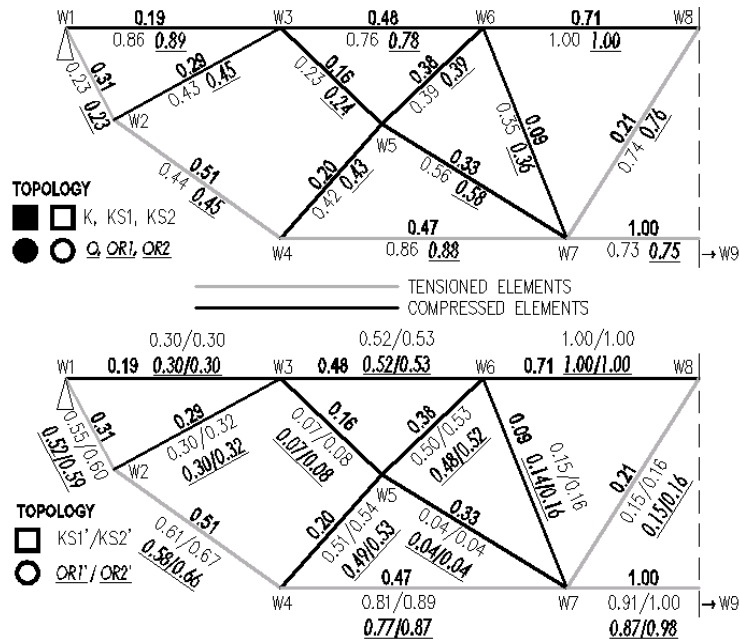


Fig. 10 Normalized cross-sectional area values of elements of topology b1 (a, b) and corresponding bars of structure B1 for *initial and constant cross sections* (a) and *reduced cross sections* (b)

The tables below show the normalized cross-sectional areas of the elements of topologies (b1, b2, b3) and the bar structures (B1, B2 and B3) for the *initial and constant cross sections* (K, KS1, KS2; O, OR1, OR2) and the *reduced cross sections* (KS1', KS2'; OR1', OR2'). A graphic comparison of the normalized cross-sectional areas is shown in the figures below. The cross-sectional area values were plotted on the symmetric halves of the truss structures and marked in the same way as the ones used in the tables. In order to make a comparative analysis possible, the cross-sectional area calculation results obtained before a material reduction were included.

When using the approximation method presented here one should bear in mind that its automatic application may result in some improper representations. No approximation algorithm improvement was used since the aim was to carry out an analysis for exactly the situation in which in some elements of the structure there is no correspondence between the cross-sectional areas for the bars obtained through topology optimization and the cross-sectional areas obtained from the standard calculations. This lack of correspondence will be the subject of further analyses.

When using the approximation method presented here one should bear in mind that its automatic application may result in some improper representations. No approximation algorithm improvement was used since the aim was to carry out an analysis for exactly the situation in which in some elements of the structure there is no correspondence between the cross-sectional areas for the bars obtained through topology optimization and the cross-sectional areas obtained from the standard calculations. This lack of correspondence will be the subject of further analyses.

Also certain problems are discussed to demonstrate how important it is to use proper optimization control parameters, a proper mass reduction coefficient and, if need be, postprocessing. Examples of problems with the mutual correspondence between cross-sectional areas are as follows:

- In the case of truss B1 one should note that bar W1-W3 was slightly deformed in the course of the computations performed using the optimization algorithm. This means that the optimization algorithm for the adopted control parameter (mass reduction coefficient and threshold function) values removed too much material from some topology bars at an insufficient available material mass. As a result such bars are weaker and their cross sections read off the topology are smaller than what the standard calculation process shows. Therefore one should remember that the results for such bars are not reliable and should be neglected in the further analysis.

- It is important to precisely determine the length of the individual bars approximated from the topology. For example, if one looks at bar W4-W7 in truss B1 and the corresponding element in topology b1 one can see that the area of node W7 in the topology is quite large and so a shorter length of the element corresponding to the bar should be tried when converting the areas for comparisons.

It follows from the above that the mutual proportions between the cross-sectional areas change. Therefore one can try other approaches to the calculations:

1. If the number of elements located on the axis of a given bar (Fig. 9(a)), per meters (in this case 14.75 m) is assumed as the length of bar W4-W7, then the bar's thickness is defined as the total number of elements per bar, divided by the determined length, i.e., 118 elements/14.75 m. In this case the bar's length was assumed as follows: for 29 elements the thickness amounts to 4 elements. There is one more column consisting of 2 elements in the left node. Therefore the bar's length was assumed as amounting to $\frac{29}{2} + \frac{2}{4} \cdot \frac{1}{2} = 14.75$.

The highest cross-sectional area value was obtained (in the same way) for bar W7-W9, calculating 230 elements/16.45 m. Then the obtained values were normalized and 1.0 for bar W7-W9 and 0.57 for bar W4-W7 were obtained while in the corresponding place in table 5.7 for the cross section calculation method without modification there is 0.47. A similar analysis was carried out for bar W2-W4, where 92 elements/11.15 m, and 0.59 was obtained, which also improves the agreement of the results with the *reduced cross sections*. Then bar W1-W2 was analyzed, in which 28 elements/4.90 m, and 0.41 was obtained (as compared with 0.31 in the table). Also in the case of bar W6-W8 one can find inconsistencies since this element's thickness amounts to 6, and even to 7 elements in some places. If a similar analysis as above is performed, there is 113 elements/11.40 m and one gets 0.83, while the table shows 0.71. It is apparent that the slightly different interpretation of the dimensions read off the topology shows better agreement between the optimization results and the actual results. It should be noted that in a certain sense it is obvious that a reduction in the amount of material (Fig. 5.9(b)) improves agreement between the results for most of the truss bars. But in the case of bar W5-W6 a deterioration occurred, due to the previously described way of determining length and to the large size of the nodes. The calculation (as above) of 46 elements/7.15 m yielded 0.46, at 0.38 in the table. This means that the agreement improved.

2. When one examines the thickness of the particular bars in Fig. 9(a), it becomes apparent that bar W6-W8 is the thickest one (its thickness amounts to 7 elements). After normalization it was assumed that this bar's relative thickness was equal to 1. The bar was used as the reference. Let us compare, for example, bar W6-W8. Let us assume that the length of this bar is measured between the blue slanting bar on the right and the yellow-brown bar on the left. In order to obtain the design length one element was added on each side (since it was necessary to fix bar W6-W8 in the node). As a result, the bar's length amounted to 16 elements/2, i.e., 8 m. The bar's average thickness of 6.375 elements was obtained as follows. All the elements along the length of 8m were counted,

Table 7 Normalized cross-sectional area values for elements of topology b2 and for corresponding bars in structure B2

| Element | Topology b2 | Initial and constant cross sections | | Reduced cross sections | | | |
|------------------------------|-------------|-------------------------------------|--------------|------------------------|-------------|-------------|-------------|
| | | K, KS1, KS2 | O, OR1, OR2 | KS1' | KS2' | OR1' | OR2' |
| W1-W2 | 0.57 | 0.18 | 0.18 | 0.48 | 0.60 | 0.38 | 0.60 |
| W2-W3 | 0.35 | 0.11 | 0.11 | 0.48 | 0.61 | 0.38 | 0.61 |
| W3-W5 | 0.81 | 0.30 | 0.30 | 0.55 | 0.69 | 0.43 | 0.69 |
| W5-W7 | 1.00 | 0.91 | 0.91 | 0.80 | 1.00 | 0.62 | 1.00 |
| W1-W4 | 0.29 | 0.76 | 0.76 | 0.37 | 0.39 | 0.33 | 0.41 |
| W4-W6 | 0.95 | 1.00 | 1.00 | 1.00 | 0.95 | 1.00 | 1.00 |
| W2-W4 | 0.22 | 0.33 | 0.33 | 0.14 | 0.17 | 0.11 | 0.17 |
| W3-W4 | 0.21 | 0.33 | 0.33 | 0.42 | 0.49 | 0.34 | 0.50 |
| W4-W5 | 0.32 | 0.19 | 0.19 | 0.18 | 0.22 | 0.14 | 0.22 |
| W5-W6 | 0.43 | 0.51 | 0.51 | 0.27 | 0.30 | 0.22 | 0.31 |
| Steel vol. [m ³] | - | 27.78 | 29.08 | 5.89 | 5.29 | 6.51 | 5.39 |

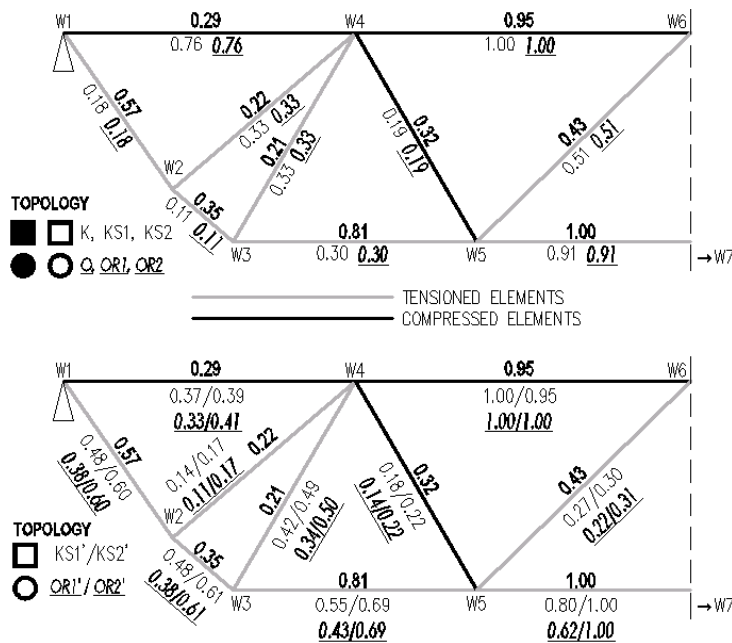


Fig. 11 Normalized cross-sectional area values of elements of topology b2 (a, b) and corresponding bars of structure B2 for *initial and constant cross sections* (a) and *reduced cross sections* (b)

i.e., $16 \cdot 2 + 6 = 102$ elements. Then this number of elements was divided by the length, i.e., $102/16 = 6.375$. This proportion relative to the thickest bar is: $6.375/7 = 0.91$ and it is much higher than the value of 0.71 shown in Table 6. This means that also in this case the agreement improved.

To sum up, depending on the way in which the design length is assumed, and so how the cross-sectional area of the particular bars is determined, different degrees of agreement between the cross-sectional areas determined from the topology and the ones calculated on the basis of the

Table 8 Normalized cross-sectional area values for elements of topology b3 and for corresponding bars in structure B3

| Element | Topology b3 | Initial and constant cross sections | | Reduced cross sections | | | |
|------------------------------|----------------|--|--------------------|------------------------|-------------|--------------------|--------------------|
| | | K, KS1, KS2 | O, OR1, OR2 | KS1' | KS2' | OR1' | OR2' |
| W1-W2 | 0.29 | 0.18 | <u>0.17</u> | 0.51 | 0.55 | <u>0.47</u> | <u>0.55</u> |
| W2-W3 | 0.56 | 0.23 | <u>0.22</u> | 0.64 | 0.69 | <u>0.59</u> | <u>0.69</u> |
| W3-W5 | 0.54 | 0.23 | <u>0.22</u> | 0.64 | 0.69 | <u>0.59</u> | <u>0.69</u> |
| W5-W8 | 0.88 | 0.28 | <u>0.28</u> | 0.74 | 0.80 | <u>0.68</u> | <u>0.80</u> |
| W8-W10 | 0.74 | 0.28 | <u>0.26</u> | 0.77 | 0.83 | <u>0.71</u> | <u>0.83</u> |
| W10-W12 | 1.00 | 0.95 | <u>0.95</u> | 0.93 | 1.00 | <u>0.85</u> | <u>1.00</u> |
| W1-W4 | 0.19 | 0.97 | <u>0.97</u> | 0.22 | 0.21 | <u>0.21</u> | <u>0.21</u> |
| W4-W7 | 0.48 | 0.39 | <u>0.38</u> | 0.47 | 0.49 | <u>0.44</u> | <u>0.49</u> |
| W7-W11 | 0.87 | 1.00 | <u>1.00</u> | 1.00 | 0.95 | <u>1.00</u> | <u>0.97</u> |
| W2-W4 | 0.16 | 0.56 | <u>0.56</u> | 0.36 | 0.37 | <u>0.34</u> | <u>0.37</u> |
| W3-W4 | 0.16 | 0.20 | <u>0.20</u> | 0.01 | 0.01 | <u>0.01</u> | <u>0.01</u> |
| W4-W6 | 0.16 | 0.11 | <u>0.11</u> | 0.12 | 0.13 | <u>0.11</u> | <u>0.13</u> |
| W5-W6 | 0.26 | 0.36 | <u>0.35</u> | 0.53 | 0.55 | <u>0.50</u> | <u>0.56</u> |
| W6-W7 | 0.22 | 0.29 | <u>0.28</u> | 0.47 | 0.48 | <u>0.43</u> | <u>0.49</u> |
| W6-W8 | 0.22 | 0.15 | <u>0.15</u> | 0.03 | 0.04 | <u>0.03</u> | <u>0.04</u> |
| W7-W9 | 0.08 | 0.10 | <u>0.10</u> | 0.12 | 0.13 | <u>0.11</u> | <u>0.13</u> |
| W8-W9 | 0.16 | 0.08 | <u>0.08</u> | 0.03 | 0.03 | <u>0.03</u> | <u>0.03</u> |
| W9-W10 | 0.16 | 0.06 | <u>0.06</u> | 0.14 | 0.14 | <u>0.12</u> | <u>0.14</u> |
| W9-W11 | 0.17 | 0.64 | <u>0.64</u> | 0.07 | 0.07 | <u>0.06</u> | <u>0.07</u> |
| W10-W11 | 0.18 | 0.72 | <u>0.72</u> | 0.16 | 0.16 | <u>0.16</u> | <u>0.16</u> |
| Steel vol. [m ³] | - | 18.54 | 19.32 | 5.44 | 5.21 | 5.59 | 5.26 |

standard are obtained. Generally, the agreement is satisfactory.

The analysis for truss B2 shows quite good agreement of the results for the *reduced cross sections* of the truss compressed bars and the topology bar cross-sectional areas of the top and bottom flanges. There is quite good agreement also as regards cross braces. For topology b2 one can see that the closer a given cross brace element is located to the midspan, the greater the thickness, whereas for bar structure B2 (Fig. 11) this is not so evident. It should be noted that in real bridge structures of this type (calculated taking into account a load moving along the girder) cross braces with a larger cross section are employed near the middle of the span. This means that as regards the tendency of the cross-sectional areas to increase, better agreement with practical bridge solutions is observed for topology b2 than for the calculations done according to the standard (truss B2). One should also note that bar W5-W6 of truss B2 was approximated from two topology bars (Fig. 9b), whereby after optimization the cross-sectional area increased and after normalization it amounted to 0.43. In the course of the analysis one could neglect the thinner bar whereby the result would be closer to the strength calculation result (equal to 0.34), as compared to 0.22-0.31 shown in the table for the reduced cross sections. This demonstrates how complex the interpretation of topology approximation for a bar structure can be. Also when determining the effective span of the bars of the trusses obtained through topology optimization one can encounter the difficulties mentioned earlier.

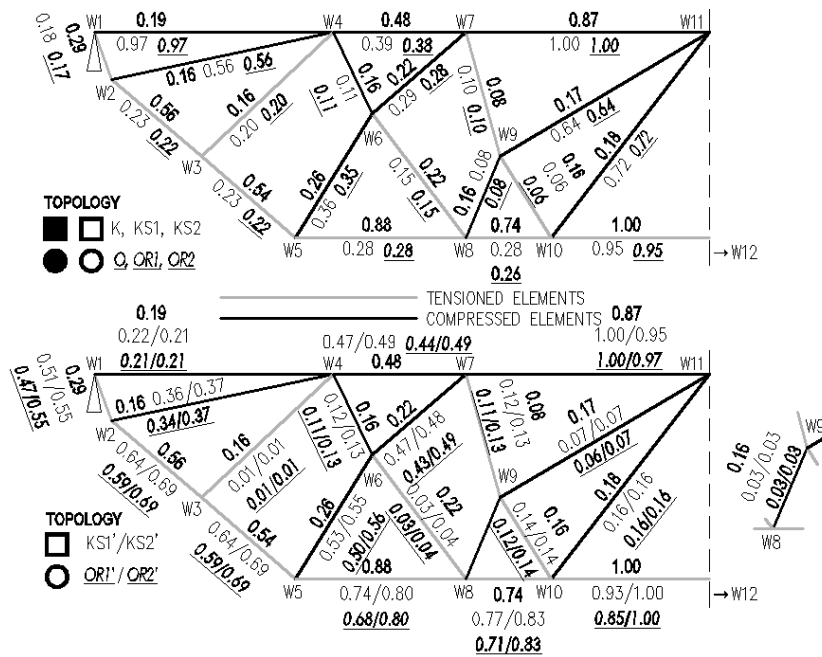


Fig. 12 Normalized cross-sectional area values of elements of topology b3 (a, b) and corresponding bars of structure B3 for *initial and constant cross sections* (a) and *reduced cross sections* (b)

As regards the *reduced cross sections* in the top flange of truss B3 (bars W1-W4, W4-W7, W7-W11), there is good agreement between the size of the cross-sectional areas, except for bar W1-W4 which cannot be included in the comparison because of the simplification applied within this bar when topology b1 was approximated into truss B1 (Fig. 4). There is also good agreement for most of the bottom flange bars. Only for bar W1-W2 the agreement is slightly poorer. When the cross-sectional areas of tensioned cross braces W3-W4 and W6-W8 were analyzed, it was found that the divergences were large for the *reduced cross sections* and smaller for the *initial and constant* cross sections. As regards the other tensioned bars (W7-W9 and W9-W10) after the reduction of the cross sections, the agreement is similar or even better. The agreement varies: sometimes it is good – as for the reduced cross sections W4-W6 and W10-W11 and sometimes poorer – as in the case of W5-W6 and W6-W7. However, if one takes into account the difficulties (mentioned earlier) in topology approximation for the bar structure and the consequent problems with deciding on the proper length for converting the topology cross-sectional areas, then the agreement can be deemed sufficient. Therefore it was decided to do the calculations again for the above bars, taking the lengths of the bars into account in a more direct way. For bar W5-W6, the division 29 elements/6.00 m yielded 0.36. The highest value of 1.0 was obtained in the same way for bar W10-W12 by dividing 240 elements/18.00 m. For bar W6-W7 the ratio of 21 elements/4.05 m yielded 0.39. To sum up, it is apparent that the approach consisting in reading bar length directly off the topology improves the agreement.

In addition, computations were performed for bars W5-W8 and W7-W11 and the agreement was found to be good, i.e., 114 elements/11.60 m and 161 elements/11.50 m yielded respectively 0.74 and 0.78, as compared with 0.88 and 0.87. In the former case (W5-W8), there was an improvement, whereas in the latter case the agreement slightly deteriorated (strength calculations

yielded 0.95-1.0). Nevertheless, if some of the finite elements belonging to bar W9-W11 and W10-W11 were taken into account, the ratio might improve. A similar conclusion emerges from an analysis of the results for bar W8-W9 where some of the material (finite elements) could be taken away from bar W8-W10. This shows that the proper allocation of finite elements is critical for very short bars.

One can notice that the highest values (1.00) for the topology and the truss girders occur in the same tensioned bottom flange elements located closest to the midspans of the trusses for the largest reduced box and pipe sections (KS2', OR2'). In the other cases the normalized cross sectional areas in the approximated elements of the trusses are very close to 1.00. The largest amounts of material were determined for the compressed top flange elements located closest to the midspans of the trusses. In the corresponding topology elements the normalized cross-sectional areas are also close to 1.00.

The normalized cross-sectional areas in the particular truss bars correspond more or less precisely to the area values in the topology elements. This is due to the fact that the loading scheme for the design area is somewhat different than that used for the approximated truss structures. Also the accuracy of approximating the topology to the bar structure and the division into finite elements may have an influence on the results. Values closer to the topology results were obtained for the reduced cross sections (KS1', KS2'; OR1', OR2') of the truss bars. Moreover, better agreement was obtained for the compressed elements, particularly in the top flange, the bottom flange and the support cross braces. In the case of the internal cross braces, the normalized cross-sectional area values sometimes differ rather significantly, which is mainly due to the adopted FE mesh.

In conclusion, topology optimization allows one to estimate the amount of material needed for the particular elements of the truss being designed. This is possible thanks to the thicknesses of the topology elements. This simplifies and speeds up the design process, especially at the conceptual stage. One should note, however, that the conversion of material amounts from the topology is somewhat troublesome and the method provided in this paper is approximate. Better agreement in the cross sectional areas between the topology and the design process can be achieved if a more accurate method of converting the amount of material in the cross section is employed.

6. Taking into account local stability of bars

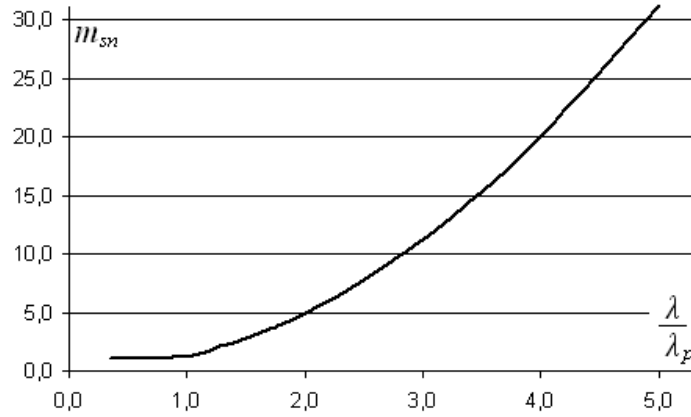
6.1 Basic assumptions

After the strength and cross-sectional slenderness conditions: $R=200$ MPa, $\lambda_{\max}=150$ (compression.), $\lambda_{\max}=200$ (tension) had been satisfied, the local stability condition was checked for the cross sections of the particular truss bars.

The box sections of girders A, B1, B2 and B3 were checked in accordance with the guidelines contained in, among others, (Code 2). The general condition of local stability under compression has this form

$$\sigma \leq \frac{R}{m_{sn}} \quad (7)$$

Coefficient m_{sn} in the above formula reduces steel strength R depending on the proportion of the dimensions of the constituent cross-sectional elements. In the considered compressed cross

Fig. 13 Coefficient m_{sn} versus relation λ/λ_p , based on (Code 2)

sections, slenderness $\lambda = \frac{b}{g} \leq \varphi \sqrt{\frac{200}{R}}$, where $\varphi=60$. This means that ultimately when

slenderness λ is smaller or equal to 60, local stability needs not to be checked for the particular elements of the compressed cross sections. Whereas when $\lambda > 60$, one should calculate coefficient m_{sn} and use formula (7) in order to determine the stresses. Coefficient m_{sn} is calculated from relation λ/λ_p which is shown in the diagram below based on the data contained in (Code 2).

Reference slenderness $\lambda_p = \frac{K}{\sqrt{R}}$, where $K=930$ (uniform compressive stress).

6.2 Effect of local stability on analyzed truss structures

6.2.1 Checking cross sections K, KS1, KS2, OR1 and OR2

The slenderness of the cross-sectional element was determined, in accordance with (Code 2), as a ratio of the wall's height inside the inner hole and the thickness of this wall. Slenderness λ was found to be above 60 for only bars W4-W6/W16-W18 and W8-W9/W13-W14 in truss B3 and cross sections KS2 (larger box sections with a size of 0.80 m). In the next step, coefficient m_{sn} was calculated for these bars. A check done for bar W8-W9/W13-W14 showed that the design strength was not exceeded. Whereas in the case of elements W4-W6/W16-W18 the strength of the steel was considerably exceeded. Therefore the cross section was increased to have the stress (with local stability taken into account) amount to 200 MPa. The cross-sectional area increased as a result of the proportional thickening of the walls.

After the changes, the cross-sectional area of bars W4-W6/W8-W9 increased by 9.11%. No other changes connected with the cross-sectional areas of the bars were observed.

The bridge standard does not include a method of determining wall slenderness for a tubular element. Therefore this was done in accordance with standard (Code 3) concerning the design of broadly understood steel constructions (regardless of their intended use or function). According to the above standard, the slenderness of the walls of tubular cross sections in compressed elements

can be determined as $\lambda = \frac{b}{g}$, where b it the tube's outer diameter and g is its wall thickness. It

was assumed that the slenderness of the cross-sectional walls of compressed tubular elements, similarly as for box sections, cannot be greater than the limit value $\lambda=60$. In the considered case, $\lambda < 60$ for all the types of structures (A, B1, B2, B3) and for any of the considered cross sections (O, OR1, OR2). The local stability relations were satisfied with a considerable margin. Thus, according to C3, the bars are resistant to local stability loss.

6.2.2 Checking cross sections KS1', KS2', OR1' and OR2'

When the local stability condition was taken into account, the steel volume increased for all the types of cross sections in all the types of trusses (A, B1, B2, B3). The increase was due to the necessity of satisfying the strength condition ($R=200$ MPa), which after taking into account local stability in bars with too thin walls was found to be not fulfilled.

The steel volume and the percentage gains and losses were compared again (taking into account local stability loss) for the trusses (B1, B2, B3) approximated on the basis of the optimization results and for the reference structure (A) used in the design process. When local stability loss was taken into account, it was found that losses occurred in most of the structures and types of cross sections. The losses are lower for smaller cross-sectional sizes (0.50 m), whereas for the size of 0.80 m they significantly increase. The increase in wall thickness for the longer total bar length (246,00 m (A), 304,37 m (B1), 273,16 m (B2), 358,19 m (B3) in the case of the B type trusses was the direct cause of the losses, which manifested themselves in the fact that ultimately slightly more steel (tab. 5.16) is needed for the trusses of type B. It should be noted, however, that for cross sections OR1' (with an outer diameter of 0.50 m) gains in steel volume were recorded for the approximated trusses B1 and B3 in comparison with reference structure A. The gains amounted to respectively 7.48 and 6.08 [%].

Table 9 Gains and losses in steel volume (after local stability was taken into account) for structures B1, B2 and B3 in comparison with typical structure A

| | Steel volume [m ³] | | | | | |
|---------------|--------------------------------|-------------|-----------------|-----------------|-----------------|-----------------|
| | K, KS1, KS2 | O, OR1, OR2 | KS1' | KS2' | OR1' | OR2' |
| A | 25.62 | 26.83 | 5.86 5.98* | 5.30 6.84* | 6.35 6.41* | 5.39 6.34* |
| B1 | 17.16 | 17.86 | 5.44 5.98* | 5.25 7.84* | 5.55 5.93* | 5.29 7.15* |
| Gain/loss [%] | 33.03 | 33.45 | 7.06 -0.13* | 0.91 -14.66* | 12.56 7.48* | 1.91 -12.82* |
| B2 | 27.78 | 29.08 | 5.89 6.14* | 5.29 7.40* | 6.51 6.61* | 5.39 6.80* |
| Gain/loss [%] | -8.42 | -8.39 | -0.65 -2.76* | 0.15 -8.20* | -2.46 -3.11* | -0.06 -7.24* |
| B3 | 18.54 18.55 [^] | 19.32 | 5.44 6.10* | 5.21 8.04* | 5.59 6.02* | 5.26 7.32* |
| Gain/loss [%] | 27.63 27.58 [^] | 28.00 | 7.04 -2.07* | 1.74 -17.66* | 11.94 6.08* | 2.50 -15.45* |

„+” – gain „-” – loss

[^] – local stability which had an effect on the results for cross sections KS2 was taken into account

* – local stability which had an effect on the results was taken into account

7. Final comparison of normalized cross sections for reference truss and trusses obtained through topology optimization

After local stability loss was taken into account it became necessary to change the proportion of elements in the cross sections in accordance with C3 and so the cross-sectional areas of the particular bars in all the considered trusses B1, B2 and B3 were calculated again.

Interesting changes can be observed in the case of truss B1. Theoretically, for the *reduced cross sections* of the compressed bars in the top flange agreement deteriorated in bar W1-W3, but this is advantageous since the amount of material in this bar needs to be increased. This means that a solution closer to reality is obtained and it also confirms the fact that even if topology optimization introduces some irregularities into the solution, they are removed. The deterioration in agreement for bar W3-W6 can be ascribed to the assumptions made for cross-sectional area conversion. The nodes in the topology are quite strongly developed and the design length is assumed to be equal to the distance between nodes. This means that even though the calculation result indicates deterioration in agreement for the assumed design length, in reality the agreement has not deteriorated if one takes the size of the nodes into account. Slightly better agreement occurred for some bars (W1-W2, W2-W4, W4-W7) in the tensioned bottom flange for cross sections KS2'. Poorer agreement was also found for some cross braces, which indicates that smaller overall dimensions should be used for bars of this type. This coincides with the trends in the design of bridge structures, where such cross sections are commonly used. Thus topology optimization has proved to be useful and the solutions obtained by means of it confirm the validity of the solutions used in the design practice.

Table 10 Normalized cross-sectional areas of elements in topology b1 and of corresponding bars B1 after changes were made when local stability loss was taken into account

| Element | Topology b1 | Initial and constant cross sections | | Reduced cross sections | | | |
|------------------------------|----------------|--|--------------------|------------------------|-------|---------------------|---------------------|
| | | K, KS1, KS2 | O, OR1, OR2 | KS1' | KS2' | OR1' | OR2' |
| W1-W2 | 0.31 | 0.23 | <u>0.23</u> | 0.55 | 0.52 | <u>0.52</u> | <u>0.59</u> |
| W2-W4 | 0.51 | 0.44 | <u>0.45</u> | 0.61 | 0.58 | <u>0.58</u> | <u>0.66</u> |
| W4-W7 | 0.47 | 0.86 | <u>0.88</u> | 0.81 | 0.77 | <u>0.77</u> | <u>0.87</u> |
| W7-W9 | 1.00 | 0.73 | <u>0.75</u> | 0.91 | 0.87 | <u>0.87</u> | <u>0.98</u> |
| W1-W3 | 0.19 | 0.86 | <u>0.89</u> | 0.37* | 0.65* | <u>0.34*</u> | <u>0.64*</u> |
| W3-W6 | 0.48 | 0.76 | <u>0.78</u> | 0.52 | 0.78* | <u>0.52</u> | <u>0.77*</u> |
| W6-W8 | 0.71 | 1.00 | <u>1.00</u> | 1.00 | 1.00* | <u>1.00</u> | <u>1.00</u> |
| W2-W3 | 0.29 | 0.43 | <u>0.45</u> | 0.37* | 0.66* | <u>0.33*</u> | <u>0.65*</u> |
| W3-W5 | 0.16 | 0.23 | <u>0.24</u> | 0.24* | 0.42* | <u>0.19*</u> | <u>0.41*</u> |
| W4-W5 | 0.20 | 0.42 | <u>0.43</u> | 0.51 | 0.78* | <u>0.49</u> | <u>0.77*</u> |
| W5-W6 | 0.38 | 0.39 | <u>0.39</u> | 0.50 | 0.78* | <u>0.48</u> | <u>0.76*</u> |
| W5-W7 | 0.33 | 0.56 | <u>0.58</u> | 0.19* | 0.33* | <u>0.15*</u> | <u>0.32*</u> |
| W6-W7 | 0.09 | 0.35 | <u>0.36</u> | 0.15 | 0.14 | <u>0.14</u> | <u>0.16</u> |
| W7-W8 | 0.21 | 0.74 | <u>0.76</u> | 0.30* | 0.52* | <u>0.25*</u> | <u>0.51*</u> |
| Steel vol. [m ³] | - | 17.16 | 17.86 | 5.98* | 7.84* | 5.93* | 7.15* |

* – local stability which had an effect on the results was taken into account

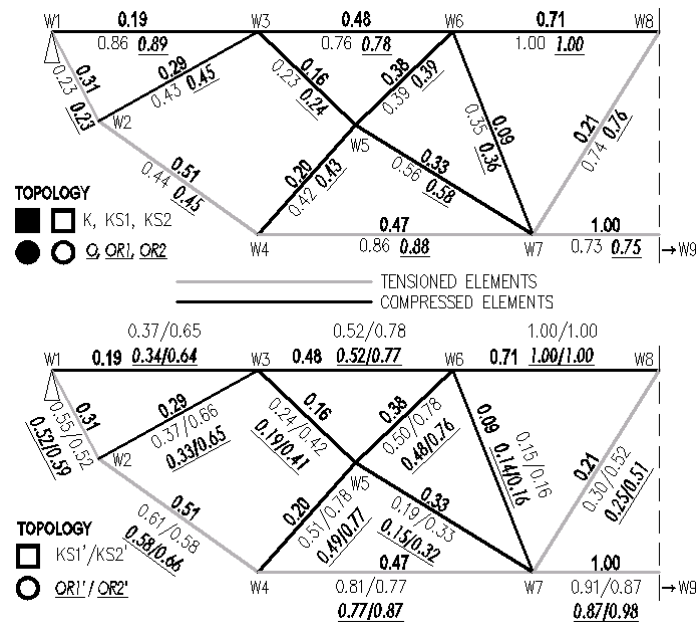


Fig. 14 Normalized cross-sectional area values of elements of topology b1 (a, b) and corresponding bars of structure B1 for *initial* and *constant cross sections* (a) and *reduced cross sections* (b) – after changes were made when local stability loss was taken into account

As regards truss B2 and the *reduced cross sections* 0.80 m in size, some negative changes in the top flange's bar W1-W4 and the bottom flange's bars W2-W3, W3-W5 and W5-W7 are noticeable. But they are small and occur in only cross sections KS2'. The changes are also due to the adopted lengths of the bars. Better agreement with the topology results is observed for the cross braces with smaller overall dimension, i.e. 0.50 m.

The results for truss B3 with the overall dimension of 0.80, similarly as for the other structures show both improved agreement (e.g. bars W2-W3, W3-W5, W8-W10) and deteriorated agreement (bars W1-W4, W4-W7, W5-W8), which is directly connected with the method of approximating the topology to a bar system (assuming locations for nodes and design lengths for the particular bars). Much better agreement was also obtained for cross brace cross-sectional areas when smaller overall dimensions were used in such bars.

The size of the particular compressed bars' cross-sectional areas changed. For most of the bars the proportions become very similar to the ones obtained for the topology. At the same time as the size of the cross sections in the internal cross braces increases, so does the normalized ratio of the cross-sectional areas, whereby it becomes less real. This means that the height of the cross braces and the cross-sectional areas should be smaller than the assumed ones. It should be noted that the topology may show the designer a better solution if he/she when looking at a given result of the optimization process with regard to truss cross braces takes into account the thickness of the particular topology elements, as both the overall dimension and the cross-sectional area. In other words, it should be noted that the topology's thin bars should not only have a smaller cross-sectional area, but also smaller overall dimensions. Then a comparison of the results will usually be more effective. This actually is the case in reality, where cross braces usually have smaller cross sections.

Table 11 Normalized cross-sectional areas of elements in topology b2 and of corresponding bars B2 after changes were made when local stability loss was taken into account

| Element | Topology b2 | Initial and constant cross sections | | Reduced cross sections | | | |
|------------------------------|-------------|-------------------------------------|-------------|------------------------|-------|--------------|--------------|
| | | K, KS1, KS2 | O, OR1, OR2 | KS1' | KS2' | OR1' | OR2' |
| W1-W2 | 0.57 | 0.18 | 0.18 | 0.48 | 0.54 | 0.38 | 0.60 |
| W2-W3 | 0.35 | 0.11 | 0.11 | 0.48 | 0.55 | 0.38 | 0.61 |
| W3-W5 | 0.81 | 0.30 | 0.30 | 0.55 | 0.62 | 0.43 | 0.69 |
| W5-W7 | 1.00 | 0.91 | 0.91 | 0.80 | 0.90 | 0.62 | 1.00 |
| W1-W4 | 0.29 | 0.76 | 0.76 | 0.37 | 0.73* | 0.33 | 0.71* |
| W4-W6 | 0.95 | 1.00 | 1.00 | 1.00 | 1.00* | 1.00 | 1.00 |
| W2-W4 | 0.22 | 0.33 | 0.33 | 0.27* | 0.55* | 0.18* | 0.53* |
| W3-W4 | 0.21 | 0.33 | 0.33 | 0.42 | 0.79* | 0.34 | 0.76* |
| W4-W5 | 0.32 | 0.19 | 0.19 | 0.18 | 0.20 | 0.14 | 0.22 |
| W5-W6 | 0.43 | 0.51 | 0.51 | 0.33* | 0.67* | 0.22 | 0.65* |
| Steel vol. [m ³] | - | 27.78 | 29.08 | 6.14* | 7.40* | 6.61* | 6.80* |

* – local stability which had an effect on the results was taken into account

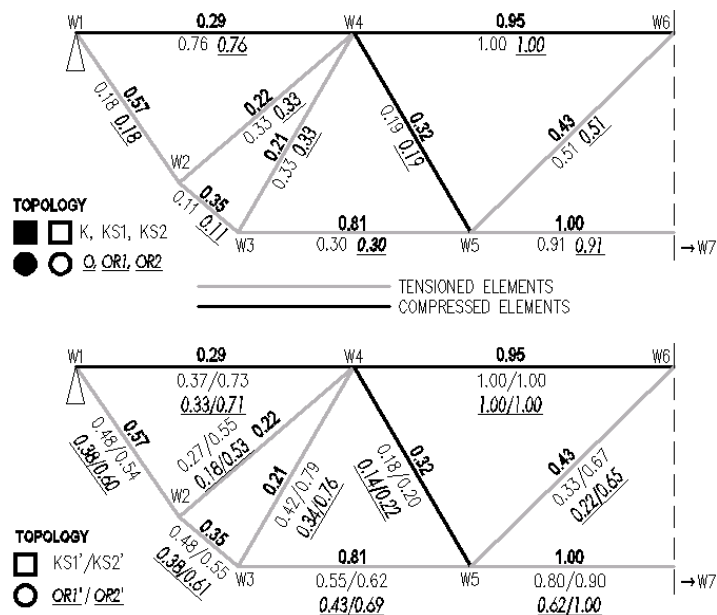


Fig. 15 Normalized cross-sectional area values of elements of topology b2 (a, b) and corresponding bars of structure B2 for initial and constant cross sections (a) and reduced cross sections (b) – after changes were made when local stability loss was taken into account

To sum up, the effect of local buckling in classic trusses carrying only axial compressive and tensile forces has a significant effect on material economy. Bridge standard C2 does not allow the use of too thin cross-sectional walls. One should also bear in mind that the open decks used in classic trusses are relatively light in comparison to the currently used ones and the one used in the considered case.

Table 12 Normalized cross-sectional areas of elements in topology b3 and of corresponding bars B3 after changes were made when local stability loss was taken into account

| Element | Topology b3 | Initial and constant cross sections | | Reduced cross sections | | | |
|------------------------------|-------------|-------------------------------------|-------------|------------------------|-------|--------------|--------------|
| | | K, KS1, KS2 | O, OR1, OR2 | KS1' | KS2' | OR1' | OR2' |
| W1-W2 | 0.29 | 0.18 | <u>0.17</u> | 0.51 | 0.50 | <u>0.47</u> | <u>0.55</u> |
| W2-W3 | 0.56 | 0.23 | <u>0.22</u> | 0.64 | 0.62 | <u>0.59</u> | <u>0.69</u> |
| W3-W5 | 0.54 | 0.23 | <u>0.22</u> | 0.64 | 0.62 | <u>0.59</u> | <u>0.69</u> |
| W5-W8 | 0.88 | 0.28 | <u>0.28</u> | 0.74 | 0.72 | <u>0.68</u> | <u>0.80</u> |
| W8-W10 | 0.74 | 0.28 | <u>0.26</u> | 0.77 | 0.75 | <u>0.71</u> | <u>0.83</u> |
| W10-W12 | 1.00 | 0.95 | <u>0.95</u> | 0.93 | 0.90 | <u>0.85</u> | <u>1.00</u> |
| W1-W4 | 0.19 | 0.97 | <u>0.97</u> | 0.34* | 0.59* | <u>0.27*</u> | <u>0.57*</u> |
| W4-W7 | 0.48 | 0.39 | <u>0.38</u> | 0.47 | 0.78* | <u>0.44</u> | <u>0.76*</u> |
| W7-W11 | 0.87 | 1.00 | <u>1.00</u> | 1.00 | 1.00* | <u>1.00</u> | <u>0.97</u> |
| W2-W4 | 0.16 | 0.56 | <u>0.56</u> | 0.42* | 0.71* | <u>0.34</u> | <u>0.69*</u> |
| W3-W4 | 0.16 | 0.20 | <u>0.20</u> | 0.01 | 0.01 | <u>0.01</u> | <u>0.01</u> |
| W4-W6 | 0.16 | 0.11 | <u>0.11</u> | 0.28* | 0.51* | <u>0.22*</u> | <u>0.49*</u> |
| W5-W6 | 0.26 | 0.36 | <u>0.35</u> | 0.53 | 0.81* | <u>0.50</u> | <u>0.79*</u> |
| W6-W7 | 0.22 | 0.29 | <u>0.28</u> | 0.47 | 0.78* | <u>0.43</u> | <u>0.75*</u> |
| W6-W8 | 0.22 | 0.15 | <u>0.15</u> | 0.03 | 0.03 | <u>0.03</u> | <u>0.04</u> |
| W7-W9 | 0.08 | 0.10 | <u>0.10</u> | 0.12 | 0.11 | <u>0.11</u> | <u>0.13</u> |
| W8-W9 | 0.16 | 0.08 | <u>0.08</u> | 0.18* | 0.32* | <u>0.14*</u> | <u>0.13*</u> |
| W9-W10 | 0.16 | 0.06 | <u>0.06</u> | 0.14 | 0.13 | <u>0.12</u> | <u>0.14</u> |
| W9-W11 | 0.17 | 0.64 | <u>0.64</u> | 0.23* | 0.41* | <u>0.19*</u> | <u>0.39*</u> |
| W10-W11 | 0.18 | 0.72 | <u>0.72</u> | 0.31* | 0.55* | <u>0.25*</u> | <u>0.53*</u> |
| Steel vol. [m ³] | - | 18.55* | 19.32 | 6.10* | 8.04* | 6.02* | 7.32* |

* – local stability which had an effect on the results was taken into account

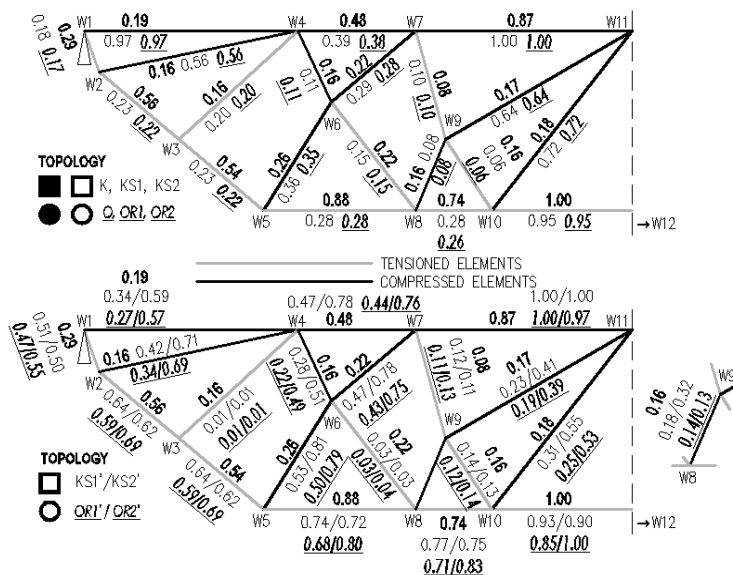


Fig. 16 Normalized cross-sectional area values of elements of topology b3 (a, b) and corresponding bars of structure B3 for initial and constant cross sections (a) and reduced cross sections (b) – after changes were made when local stability loss was taken into account

The above calculations showed how important role the proper mapping of the topology into the truss plays. It was demonstrated that when there are no gains in material consumption this is mainly due to the adopted assumptions simplifying the truss as compared to the topology. The analysis was carried out to show the complexity of the problem and that the development of proper calculation procedures is a complicated task.

8. Conclusions

The possibilities of the practical application of the optimization algorithm in conceptual design have been demonstrated. Conceptual design is often the most important stage in the design process, during which the basic overall dimensions of the structure and the needed amounts of material are determined and the economics of individual solutions are assessed.

The analysis was carried out for steel bridge trusses under the standard load. The effect of buckling was taken into account and thoroughly examined. Comparisons were made for three different approximated trusses and a typical girder used in design practice. Also different types of cross sections were considered.

Structures more optimal than the typical ones can be obtained through optimization. When buckling is taken into account, the stress level in the individual elements may be lower in the approximated girders than in the typical girder designs.

Topology optimization can also be helpful in assessing the amount of material needed for the particular elements of the truss girder, whereby the design process can be significantly shortened.

Also buckling may have a smaller effect (than the one determined in this work) in trusses obtained by means of the optimization algorithm, due to the fact that larger nodes, and consequently shorter reduced buckling lengths of the bars, occur in the obtained topologies.

The above calculations were made for a linear case. In the case of geometrical and/or material nonlinearity, the optimal topology will be slightly different, since in such cases the structures are stiffer (Huang and Xie 2010), and the total amount of material can be slightly larger. In the linear case, the amount of material needed may be the same or even smaller when stronger inclusions are added (Kutyłowski 2009).

Trusses with a deck of the same type as the one considered in this work are designed today, but the way in which the load from the deck is applied to the truss is different: the deck is fixed to the truss's top flange in a continuous way whereby besides axial forces also bending moments and shearing forces occur in the truss. Appropriate calculations have been just completed and the obtained results are promising.

References

- Bendsøe, M.P. (1989), "Optimal shape design as a material distribution problem", *Struct. Optim.*, **1**(4), 193-202.
- Bendsøe, M.P. and Sigmund, O. (1999), "Material interpolation schemes in topology optimization", *Arch. Appl. Mech.*, **69**(9-10), 635-654.
- Bendsøe, M.P. and Sigmund, O. (2003), *Topology optimization, theory, methods and applications*, Springer, Berlin Heidelberg New York.
- Guedes, J.M. and Taylor, J.E. (1997), "On the prediction of material properties and topology for optimal continuum structures", *Struct. Optim.*, **14**(2-3), 193-199.

- Huang, X. and Xie, Y.M. (2010), "Evolutionary topology optimization of geometrically and materially nonlinear structures under prescribed design load", *Struct. Eng. Mech.*, **34**(5), 581-595.
- Kmita, J., Bień, J. and Machelski., Cz. (1989), *Komputerowe wspomaganie projektowania mostów (Computer aided bridge design)*, WKiŁ, Warsaw.
- Kutylowski, R. (2002), "On nonunique solutions in topology optimization", *Struct. Mult. Optim.*, **23**(5), 398-403.
- Kutylowski, R. and Rasiak, B. (2008), "Influence of various design parameters on the quality of optimal shape design in topology optimization analysis", *Proceedings in Applied Mathematics and Mechanics (PAMM)*, **8**, 10797-10798.
- Kutylowski, R. (2009), "Topology optimization of the structure using multimaterial inclusions", *Struct. Eng. Mech.*, **33**(3), 285-306.
- Lee, E.H. and Park, J. (2011), "Structural design using topology and shape optimization", *Struct. Eng. Mech.*, **38**(4), 517-527.
- Niu, B., Yan, J. and Cheng, G. (2009), "Optimum structure with homogeneous optimum cellular material for maximum fundamental frequency", *Struct. Mult. Optim.* **39**(2), 115-132.
- Ramm, E., Bletzinger, K.U, Reitingner, R. and Maute, K. (1994), "The challenge of structural optimization", *Advanced in Structural Optimization (Int. Conf. on Computational Structures Technology held in Athen)*, Eds. Topping, B.H.V. and Papadrakakis, M., 27-52.
- Code 1 PN-85/S-10030, *Obiekty mostowe, Obciążenia*, (Bridges. Loading).
- Code 2 PN-82/S-10052, *Obiekty mostowe, Konstrukcje stalowe, Projektowanie*, (Bridges. Steel structures. Designing).
- Code 3 PN-90/B-03200, *Konstrukcje stalowe, Obliczenia statyczne i projektowanie*, (Steel Structures. Static calculations and designing).